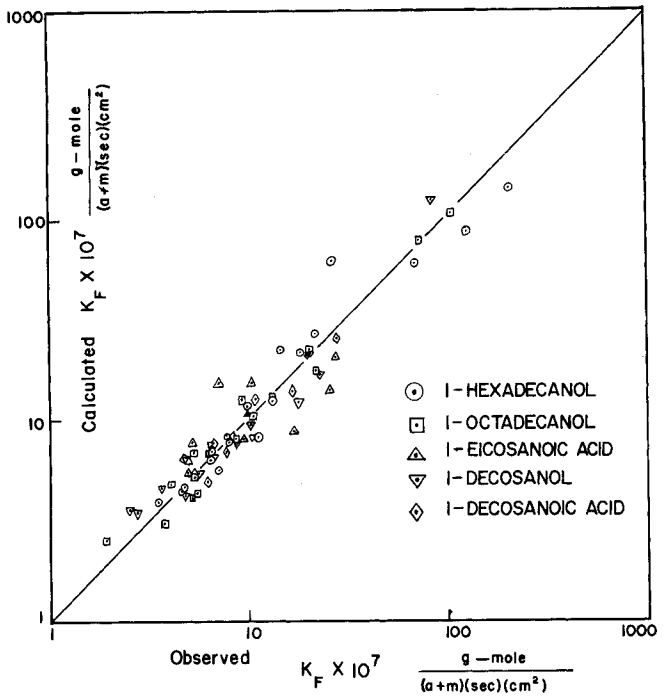

Fig. 3. Comparison of the observed and calculated mass transfer coefficient. (Data for carbon dioxide-monolayer systems included).

the local coefficient will be very close to that of the average value based on the entire surface area. When the area coverage per molecule is increased further, the distribution of void areas in the film becomes irregular. Eventually, the film breaks away and forms islands which cover part of the water surface. Under this condition, the local coefficient can be quite different from the average value because of its dependence on the sampling location. The choice of the ranges of applicability for Equation (1) is somewhat arbitrary and is based on the experimental data. It will be of value if the above observations are verified experimentally.

CONCLUSIONS

A correlation has been proposed for the transport of gases through insoluble monolayers in the form of Equation (1). This equation is applicable to an area coverage below 32Å.²/molecule of the monolayer and when interactions among molecules of water, gas, and monolayer may be neglected. Therefore, it is suggested that the correlation should be applied only to slightly soluble gases and at high surface pressure of the film where the monolayer molecules are highly compacted. If information is available on the molecular size of the monolayer, then the actual void area in the film can be calculated. By also taking into consideration the interactions among molecules, we may very well be able to correlate all the systems by a single equation. However, this can be done only after the structure of the monolayer molecules and their interactions with water and gas are fully understood.

ACKNOWLEDGMENT

The author is grateful to Professor D. M. Himmelblau for making available to him the detailed data reported in the original paper.

NOTATION

a, b, c = empirical constants, defined by Equation (1)
A = area per molecule, Å.²/molecule
k_F = interphase mass transfer coefficient in monolayer, g.-mole/(atm.)(sq.cm.)(sec.)
r = radius of gas molecule, Å.
S_a, S_b, S_c = standard error of partial regression coefficients
t = Student's t

LITERATURE CITED

1. Perry, J. H., "Chemical Engineers' Handbook," 4th Ed., pp. 3, 4, 14 to 20, McGraw-Hill, New York (1963).
2. Sada, E., and D. H. Himmelblau, *AIChE J.*, 13, 860 (1967).
3. Walker, D. C., *Rev. Sci. Instr.*, 34, 1006 (1963).

Optimal Control Profile Specification for Boundary Value Systems

J. T. BALDWIN and L. D. DURBIN

Texas A&M University, College Station, Texas

Very little interest has been shown in the problem of specifying the optimal control profile for a second-order system with boundary conditions. Important systems involve space distribution with backmixing or recycle. The flow reactor with axial dispersion has been studied only with respect to specification of optimal isothermal conditions (*1*) and the temperature profile which maximizes the product yield for a single reversible reaction (*5*). Here, a general second-order system is analyzed for optimal control profile specification and applied in a study of the axial dispersion reactor with a series of first-order reactions.

The problem under consideration concerns the specification of a control profile vector $\mathbf{u}(z)$, such that the performance index J is maximimized where

$$J(\mathbf{u}) = \int_0^1 L(\mathbf{y}, \mathbf{u}, z)\, dz \qquad (1)$$

subject to the set of nonlinear second order differential state equations and boundary conditions for $j = 1$ to J as follows:

$$\ddot{y}_j - c_j\dot{y}_j + c_j r_j(\mathbf{y}, \mathbf{u}) = 0 \qquad (2)$$

$$-c_j^{-1}\dot{y}_j(0) + y_j(0) = y_j^o \qquad (3)$$

$$\dot{y}_j(1) = 0 \qquad (4)$$

The variables $y_j(z)$ may be such variables as pressure, temperature, or composition which determine the state of the process at any position z. The rate terms r_j are determined by the state of the system at any position z. The objective function J is indicated as a function only of the control vector $\mathbf{u}$ since specification of $\mathbf{u}$ determines the state vector $\mathbf{y}$ by Equations (2) to (4).

The second-order differential Equations (2) may be reduced to $I = 2J$ first-order differential equations by specifying new state variables, x_i, such that

$$x_{2j-1} = y_j \quad \text{and} \quad x_{2j} = \dot{y}_j \qquad (5)$$

J. T. Baldwin is with Union Carbide Corporation, South Charleston, West Virginia.

to obtain

$$\dot{x}_i = g_i(\mathbf{x}, \mathbf{u}, z) = 0 \quad \text{for} \quad i = 1 \text{ to } I \tag{6}$$

where

$$g_{2j-1} = x_{2j} \quad \text{and} \quad g_{2j} = c_j x_{2j} - c_j\ r_j \tag{7}$$

The boundary condition Equations (3) and (4) may be reduced in the same manner. These boundary condition equalities are further specified as inequality constraints in the form:

$$p_i(0) = p_i\,[\mathbf{x}(0)] \leqq 0 \tag{8}$$

and

$$q_i(1) = q_i\,[\mathbf{x}(1)] \leqq 0 \text{ for } i = 1 \text{ to } I \tag{9}$$

Thus, in the new state variables the pair of inequality constraint functions;

$$p_{2j-1} = -\,c_j^{-1}\ x_{2j}(0) + x_{2j-1}(0) - x^o_{2j-1} \quad \text{and} \quad p_{2j} = -\,p_{2j-1} \tag{10}$$

and the pair:

$$q_{2j-1} = x_{2j}(1) \text{ and } q_{2j} = -\,q_{2j-1} \tag{11}$$

respectively imply Equations (3) and (4) for $j = 1$ to J. The problem now is to specify $\mathbf{u}(z)$ in order to maximize J subject to Equations (5) to (9).

If the state and control variables, $\mathbf{x}$ and $\mathbf{u}$, are unconstrained, necessary conditions for max J are determined by the Euler-Lagrange equations in the Lagrange multipliers or the adjoint or costate variables, λ_i. These are normally obtained by adjoining the differential equations to the integrand, L, in J; integrating by parts; and setting the first-order variations of J from optimal conditions with respect to each x_i and u_m equal to zero. Each boundary condition constraint specified in Equations (8) and (9) is also adjoined to J with respective constant multipliers μ_i and ν_i for $i = 1$ to I. The necessary conditions for optimality result by specifying conditions that decrease the variation in J about the optimal conditions to zero if possible. Thus, the adjoint equations result for $i = 1$ to I as

$$\dot{\lambda}_i = -\frac{\partial H}{\partial x_i} \tag{11}$$

with boundary conditions specified by

$$\lambda_i(0) = \sum_{k=1}^{I} -\mu_k \frac{\partial p_k(0)}{\partial x_i(0)};\ \lambda_i(1) = \sum_{k=1}^{I} \nu_k \frac{\partial q_k(1)}{\partial x_i(1)} \tag{12}$$

where the Hamiltonian function is given by

$$H(\mathbf{x}, \mathbf{u}, \boldsymbol{\lambda}) = L + \sum_{i=1}^{I} \lambda_i g_i \tag{13}$$

According to Pontryagin's (*10*) maximum principle, the choice of the control vector, $\mathbf{u}$, for optimal conditions is such that H is a maximum. Mangasarin (*8*) gives further conditions which are sufficient for a maximum in J relevant to conditions of differentiability and convexity of the L, g_i, $p_i(0)$, and $q_i(1)$ functions. In many practical situations, the sufficient conditions are not known beforehand. Coward and Johnson (*4*) give examples of multiple and unacceptable solutions which satisfy the maximum principle. Thus, the sufficiency of results must be established in each case to the satisfaction of the user.

Between successive pairs ($i = 2j - 1$ and $i = 2j$) of the adjoined boundary conditions, the μ and ν multipliers may be eliminated for $j = 1$ to J. Further each successive pair of differential and boundary condition equations may be combined after differentiating those with $i = 2j$. Thus, in terms of a new adjoined variable $\rho_j = \lambda_{2j}$ for $j = 1$ to J in $0 \leqq z \leqq 1$:

$$\ddot{\rho}_j + c_j\dot{\rho}_j + \sum_{k=1}^{J} c_k \left(\frac{\partial r_k}{\partial y_j}\right) \rho_k = \frac{\partial L}{\partial y_j} \tag{14}$$

with the boundary conditions

$$\dot{\rho}_j(0) = 0 \qquad \text{at } z = 0 \tag{15}$$

and

$$\dot{\rho}_j(1) + c_j\rho_j(1) = 0 \text{ at } z = 1 \tag{16}$$

The methods of specifying the distributed control to achieve an optimal boundary value system are applied to the problem of specifying the temperature profile $u(z) = T(z)$ to achieve maximum product yield in a flow reactor with axial mixing. The reactor is considered to be of normalized length, perfectly mixed in the radial direction but with uniform eddy-diffusivity, D, in the axial direction characterized by the Peclet number, N_{Pe}. A series of first-order reactions of the form:

$$A \xrightarrow{k_1} R \xrightarrow{k_2} S \tag{17}$$

is assumed to occur within the reactor with rates of appearance of A and R given by

$$r_A = -\,\alpha_1\ y_A \quad \text{and} \quad r_R = \alpha_1\ y_A - \alpha_2\ y_R \tag{18}$$

Turbulent mixing is assumed to be dominant, equal diffusivities are assumed for all reaction and product components in Equation (17). The diffusion model of this reactor is characterized by component material balances which take the form of Equations (2) to (4) where $J = 2$ and $j = 1, 2$ refers to components A and R, respectively. Also, y_j and y_j^o are the composition ratios at position z and at the inlet ($z = 0^-$), respectively. Similarly, r_j is the expression for the rate of appearance of component j. Here, a reactor of unit uniform cross-sectional area and unit space time $\tau = V/v$, is assumed.

Calculations have been made to specify the temperature profile $u(z) = T(z)$ which maximizes the yield of the intermediate product R in the axial dispersion reactor with the first order reaction sequence given by Equation (17). The inlet feed conditions are given as $y_1^o = 0.95$ and $y_2^o = 0.05$. The performance index becomes

$$J = y_2(1) - y_2^o = \int_0^1 r_2\ dz \tag{19}$$

The differential Equations (2) and the boundary conditions, Equations (3) and (4), are applicable and allow J to be stated in terms of the integrated rate of appearance of R. Thus, the rate of appearance of R should be maximized at each point along the reactor. The reactor with axial dispersion such that $N_{Pe} = 5$ is considered. Otherwise, the rate expressions are the same as those given by Bilous and Amundson (*3*) in their study of optimum temperature gradients in plug flow reactors. These are Equations (18) with

$$\alpha_1 = 5.35 \times 10^{11} \exp(-\,9{,}059\ u^{-1})$$

and

$$\alpha_2 = 4.61 \times 10^{18} \exp(-\,15{,}098\ u^{-1})$$

The control variable $u(z)$ influences relative rates of appearance of components A and R through the exponential dependence upon the reciprocal of the temperature.

THE BACKFLOW CELL MODEL

For calculational purposes, the backflow cell model (*2, 9*) of the axial diffusion reactor system will be employed here as the means of obtaining digital solutions. As indi-

cated by Figure 1, the model is assumed to consist of a series of perfectly mixed cells of equal volumes, $V_k = V/N$, with backflow between adjacent cells determined by the backflow ratio, β. The material balance equations for components $A = 1$ and $R = 2$ about an arbitrary kth cell are, respectively:

$$(1+\beta_k)y_{1,k-1} - (1+\beta_k+\beta_{k+1})y_{1,k} + \beta_{k+1}\, y_{1,k+1} + r_{1,k} = 0$$
$$(1+\beta_k)y_{2,k-1} - (1+\beta_k+\beta_{k+1})y_{2,k} + \beta_{k+1}\, y_{2,k+1} + r_{2,k} = 0 \quad (20)$$

Here, for the first cell, set $k = 1$ and let $y_{1,0} = y_1^o$ and $y_{2,0} = y_2^o$ with $\beta_1 = 0$. For the last or Nth cell, set $k = N$ and set $\beta_{N+1} = 0$. The specification of the interior β's is made such that the phi number, ϕ, equals the Peclet number, N_{Pe}, for uniform cell volumes and axial mixing conditions. The correspondence between the steady state results for the two models has been previously given (2, 9). Here, the effect of cell size is further investigated for methods of optimal profile calculations.

If the temperature, u_k, of each cell is specified, the backflow cell model Equations (20) are linear in the composition variables $\{y_{j,k}\}$ for the first-order reaction. If the $2N$ equations are arranged sequentially for component A and R for cells 1 to N, then a quidiagonal matrix equation can be written as:

$$\mathbf{A}\ \mathbf{Y} = -\mathbf{Y}^o \quad (21)$$

In this case, the column vector of composition values becomes

$$\mathbf{Y} = \text{col. } \{y_{1,1};\ y_{2,1};\ y_{1,2} \ldots y_{1,k};\ y_{2,k};\ \ldots y_{1,N};\ y_{2,N}\}$$

and the inlet feed composition vector is $\mathbf{Y}^o = \text{col. } \{y_1^o,\ y_2^o,\ 0,\ \ldots\ 0,\ 0\}$. The quidiagonal coefficient $\mathbf{A}$ matrix is specified with diagonals designated from left to right with elements, a, b, c, d, and e, respectively, with the major diagonal along the diagonal of c elements. The elements corresponding to the kth cell are on the nth and $(n+1)$th rows and are specified for uniform β's by

$$a_n = a_{n+1} = 1+\beta;\ b_n = 0;\ b_{n+1} = \alpha_1^*;$$
$$c_n = -(1+2\beta+\alpha_1^*);$$
$$c_{n+1} = -(1+2\beta+\alpha_2^*);$$
$$d_n = d_{n+1} = 0;\ e_n = e_{n+1} = \beta \quad (22)$$

Here, $\alpha^* = \alpha/N$ is the space-rate constant for a cell. Gaussian elimination (9) is used to solve the quidiagonal system to obtain $\mathbf{Y}$ for a specified temperature profile, $\{u_k\}$.

The Hamiltonian is defined by Equation (13) with $L = r_2(y_1, y_2, u)$ and $c_j = N_{Pe}$. The system of second-order adjoint equations for $J = 2$ is given by Equation (14) with boundary condition Equations (15) and (16). Each second-order differential Equation (14) may be represented in a discrete approximation by a backflow cell model with net flow in the reverse direction as indicated by Figure 2 with the state of each cell defined by the co-state variables. The zero net flow into or out of the stream of cells approximates the boundary conditions, Equations (15) and (16). The typical equations for the kth cell with $2 \leq k \leq (N-1)$ take the form:

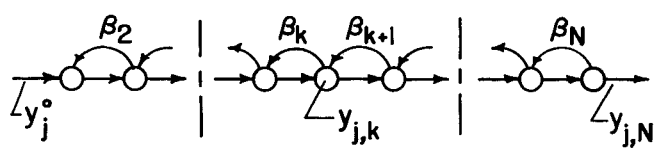

Fig. 1. The backflow cell model of state equations.

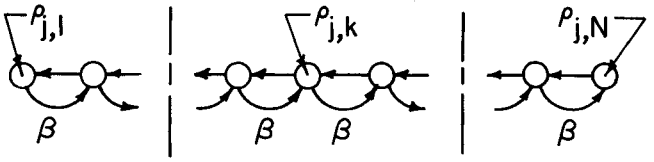

Fig. 2. The backflow cell model of adjoint equations.

$$\beta\rho_{j,k-1} - (1+2\beta)\rho_{j,k} + (1+\beta)\rho_{j,k+1} + \sum_{i=1}^{2}\left(\frac{\overline{\partial r_j}}{\partial y_i}\right)_k \rho_{j,k} = N_{Pe}^{-1}\left(\frac{\overline{\partial r_2}}{\partial y_j}\right)_k \quad (23)$$

for $k = 1$, set $\rho_{j,0} = 0$ and for $k = N$, set $\rho_{j,N+1} = 0$ to obtain the complete set of equations. It is assumed that the values of the state variables $\{\overline{y}_{j,k}\}$ and the control profile $\{\overline{u}_k\}$ are known as indicated by the bar over the partials. Then, the adjoint equations are linear in the co-state variables $\{\rho_{j,k}\}$. The adjoint equations can be written directly as a quidiagonal matrix equation in the form:

$$\mathbf{A}^T\ \mathbf{P} = \text{"}\mathbf{I}^{\bullet o} \quad (24)$$

The co-state column vector is $\mathbf{P} = \{\rho_{j,k}\}$ for alternating $j = 1, 2$ for $k = 1$ to N and the constant column vector is "$\mathbf{I}^{\bullet} = N_{Pe}^{-1}\{\alpha_1^*, -\alpha_2^*, \alpha_1^*, -\alpha_2^*, \text{ etc.}\}$ with $2N$ entries. Here, the quidiagonal coefficient $\mathbf{A}^T$ matrix has the same elements of Equation (22) but with the element transposed in the array. The matrix Equation (24) may be solved, as noted previously, to yield the costate vector, $\mathbf{P}$.

METHODS OF SUCCESSIVE APPROXIMATION TO THE OPTIMAL CONTROL PROFILE

Gradient methods were used to successively improve the control (temperature) profile. These are based upon the use of the backflow cell model concept for both the state and adjoint equations. First, for an assumed constant control (temperature) profile, the state Equation (21) is solved for the state profile, $\mathbf{Y} = \{y_{j,k}\}$, and then the co-state variables, $\mathbf{P} = \{\rho_{j,k}\}$, are obtained by solution of Equation (24). The gradient of the Hamiltonian is obtained from the computed state and costate values for each cell as

$$\left.\frac{\partial H}{\partial u}\right|_k = N\left\{(1-\overline{\rho}_2\ N_{Pe})\left[\overline{y}_1\left(\frac{\overline{\partial\alpha_1^*}}{\partial u}\right) - \overline{y}_2\left(\frac{\overline{\partial\alpha_2^*}}{\partial u}\right)\right] + N_{Pe}\overline{\rho}_1\ \overline{y}_1\left(\frac{\overline{\partial\alpha_1^*}}{\partial u}\right)\right\}_k \quad (25)$$

Then, the next assumed control profile, $\{\overline{u}_k\}$, is determined and the process repeated until the composition change in each cell becomes negligible or $|\Delta y_{j,k}| \leq \epsilon$.

The speed of convergence was studied for three types of gradient methods. In general, the $(h+1)$th approximation to the optimal control value, u_k, for a cell is determined by

$$u_{k,h+1} = u_{k,h} - \sigma_h\left[\left.\frac{\partial H}{\partial u}\right|_{k,h} + s_{k,h}\right] \quad (26)$$

The usual steepest ascent method (11), noted as Method I, here, is obtained when $s_{k,h} = 0$ and the gradient weighting factor, $\sigma_h = \sigma$, is a constant specified for all iterations. Here, Method II is the steepest ascent method with σ_h automatically reset for each iteration. The choice of σ_h is that which maximizes the yield or J. The search method is initiated by varying σ in increments of 500 until the maximum in J is bounded within an interval of 1,000. This is used as the starting interval for a Fibonacci search

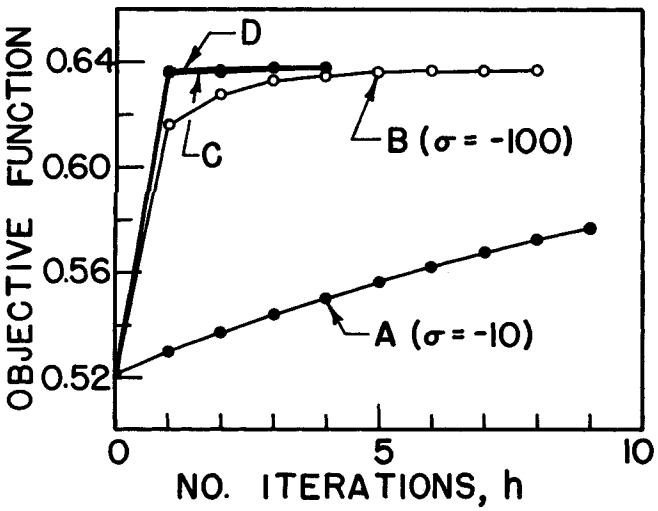

Fig. 3. Convergence of successive approximations. Curves (method): A and B (I); C (II); D (III).

(12) to decrease the bound to an interval of 20. Then, the last three points are used in a quadratic fit to give the approximate value of σ_h for a maximum in J. This same technique of specifying σ_h is used in Method III, the conjugate gradient method (7) which includes the influence of previous iterations in $s_{k,h}$ according to

$$s_{k,h} = \left(\frac{\partial H}{\partial u}\bigg|_{k,h-1} + s_{k,h-1} \right) \times \left[\int_0^1 \left(\frac{\partial H}{\partial u} \right)_h^2 dz \Big/ \int_0^1 \left(\frac{\partial H}{\partial u} \right)_{h-1}^2 dz \right] \quad (27)$$

DISCUSSION AND CONCLUSIONS

The results of the numerical study are shown by Figures 3 to 8. In Figure 3, the variations of the performance function J with the number of approximations to u for the three gradient methods are shown for ten cells. In all cases, an initial isothermal temperature profile of 350°K. was assumed. Methods II and III indicate that a very effective relaxation parameter σ_h can be estimated even for the second estimate of $\{u_k\}$. Also, both of these methods are almost equivalent with a slight edge given to the conjugate gradient method. As indicated, the usual steepest ascent method with prior specification of the constant relaxation or step length factor, $\sigma = \sigma_h$, converges slowly depending upon the value of the factor selected.

The variation of J with σ is indicated by Figure 4 after the first gradients are calculated for the ten cell case. With

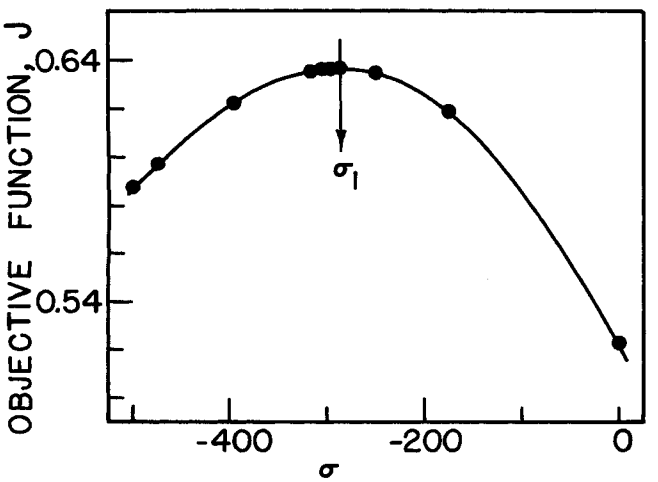

Fig. 4. Performance index variation with relaxation parameter. For 10 cells after initial approximation of u.

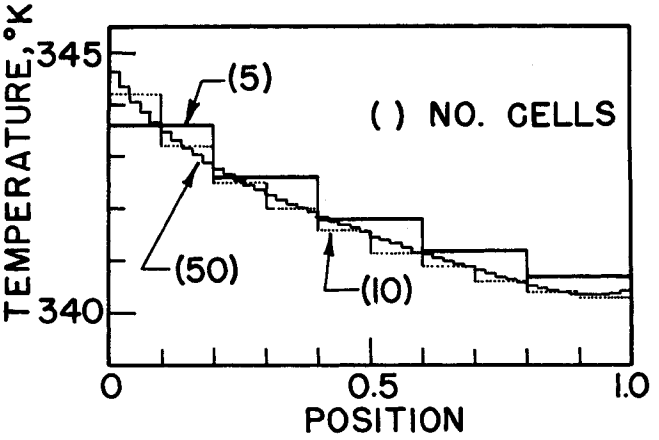

Fig. 5. Optimal temperature profiles.

Methods II and III, the selected value of the relaxation parameter for the next step is $\sigma_1 = -287.1$. The points indicate the ten steps taken in the search for the maximum. Each of these points requires a new solution of the state Equations (21). This is the price that must be paid for the use of this method. This would become more critical for nonlinear reaction systems which would require iterative methods of solving the state equations. However, the method of automatically specifying the relaxation parameter would be quite useful for previously unexplored problems. Oftentimes (11), too large a value of $|\sigma|$ will cause a problem to become unstable and diverge and too small a value means slow convergence. The effect of the procedure given by Methods II and III above is to select the best step size factor for each successive approximation. As more knowledge is gained about a problem, the search for the optimum σ on each successive approximation can be made more efficient with corresponding savings in computer time.

All of the results that are presented in Figures 5 to 8 were obtained after convergence was obtained as determined by each $|\Delta y_{j,k}| \leq 10^{-5}$. Here, $\Delta y_{j,k}$ is the difference between successive estimates of the optimal composition value for component j in the kth cell. In Figure 5, the optimal temperature profiles are shown for 5 cells with $\beta = \frac{1}{2}$, for 10 cells with $\beta = 1.5$, and for 50 cells with $\beta = 9.5$ corresponding to $N_{Pe} = 5$. Towards the end of the reactor the temperature for 5 cells lies above and that for 10 cells lies below the profile for 50 cells. It is inter-

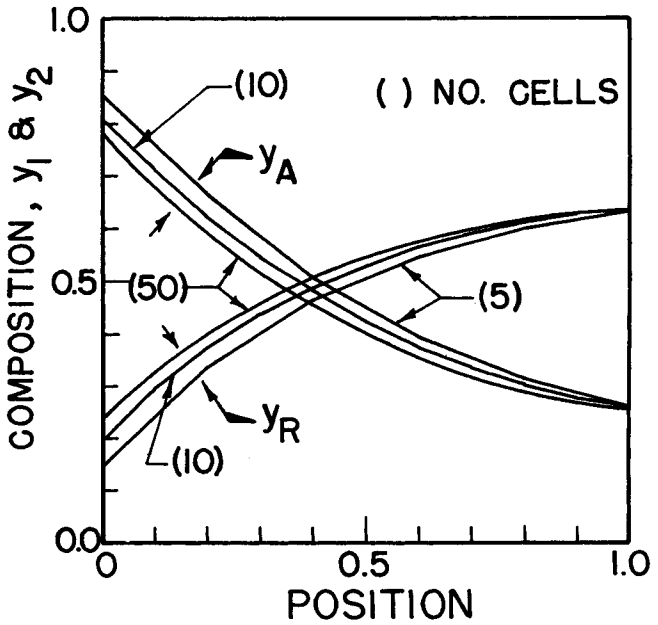

Fig. 6. Optimal composition (state) profiles.

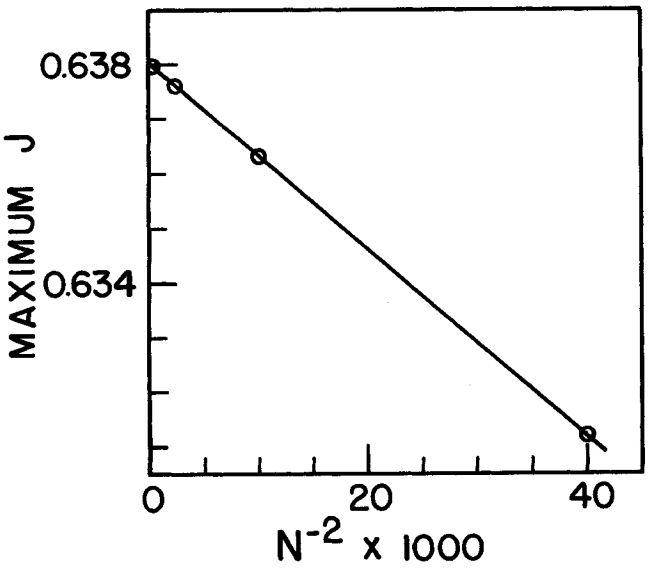

Fig. 7. Variation of optimum yield with number of cells.

esting to compare these with the results given by Bilous and Amundson (3) for the same reactions in a plug flow reactor. They found the maximum yield to be $y_2(1) = 0.685$ and their temperature profile falls off very sharply in the first two-tenths of the reactor to about 341°K. and levels off to reach 335.6°K. at the end. The addition of axial dispersion results in a much flatter profile starting at lower temperatures right after the inlet. For example, for 50 cells with $\beta = 9.5$ the temperature at $z = 0^+$ is 344.8°K. for a smooth curve through the stairstep plot. This lower initial temperature is related to the jump discontinuity in the compositions $y_1(0)$ and $y_2(0)$ right after the inlet. The curves of the optimal composition profiles displayed by Figure 6 for 5, 10, and 50 cells show the effect of backmixing and finite differencing (or cell size). The straight line variation of the maximum intermediate yield $y_R(1) = y_2(1)$ with N^{-2} shown by Figure 7 allows extrapolation to $N \rightarrow \infty$. This gives an estimate of 0.638 for the continuous diffusion model. This indicates that the N^{-2} extrapolation of the maximum value of the performance function is a useful consideration to be used with the backflow cell model as a discrete analog of the continuous dispersion model. The variation of the adjoint

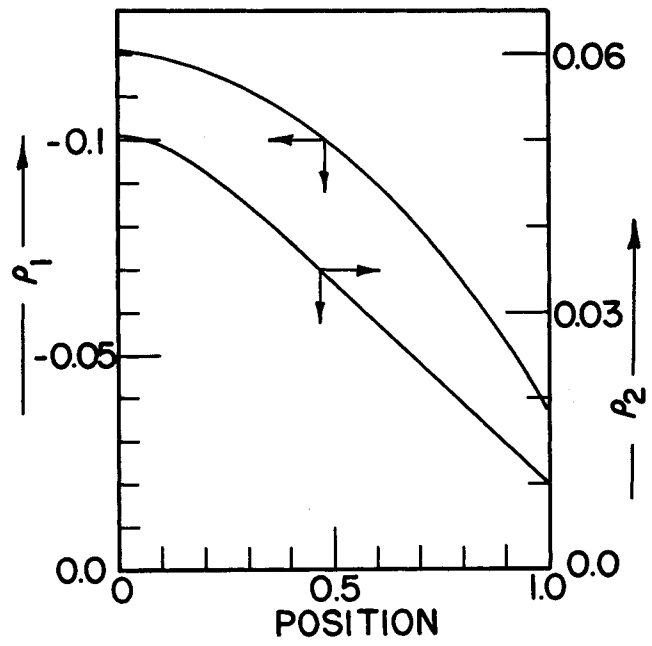

Fig. 8. Optimal costate profiles for 50 cells.

or co-state variables with position along the reactor approximated by 50 cells is given by Figure 8. It should be noted that ρ_1 is negative and increases but that ρ_2 is positive and decreases along the reactor. This is contrary to the situation for plug flow which has the adjoint variables increasing with position and becoming zero at the outlet. An example of this is shown by Fine and Bankoff (*6*). Here, the second-order adjoint variables exhibit the jump discontinuity at $z = 1$ due to boundary condition Equation (16).

ACKNOWLEDGMENT

L. D. Durbin acknowledges the partial support of the D.O.D. Project Themis-Optimization Studies at Texas A&M University. J. T. Baldwin appreciates the support of an Alcoa Foundation Fellowship. The aid of the Texas Engineering Experiment Station with the digital computation is acknowledged.

NOTATION

c_j = constant coefficient, N_{Pe} for case studied
D = eddy diffusivity, sq.ft./hr.
J = performance index or objective function
k = first-order rate constant, hr.$^{-1}$
N_{Pe} = Peclet number, vV/D for unit cross-sectional area
N = number of cells in backflow cell model
r_j = rate of appearance of component j
u = control function
v = volumetric flow rate, cu.ft./hr.
V = total volume of flow system of unit cross-sectional area, cu.ft.
z = normalized length of the flow system

Greek Letters

α = space time-rate constant, $k\tau$
β = backflow ratio of backflow rate to forward flow rate
λ = adjoint variables relative to state vector x
ρ = adjoint or costate variables relative to y vector
σ = relaxation parameter in gradient method
τ = total space time, V/v = unity here
ϕ = phi number, $2N/(1 + 2\beta)$

Subscripts

h = hth successive approximation
i = state variable index
j = component or second-order state variable index
k = arbitrary cell number

LITERATURE CITED

1. Adler, J., and D. Vortmyer, *Chem. Eng. Sci.*, **18**, 99 (1963).
2. Baldwin, J. T., and L. D. Durbin, *Can. J. Chem. Eng.*, **44**, 151 (1966).
3. Bilous, O., and N. R. Amundson, *Chem. Eng. Sci.*, **5**, 115 (1956).
4. Coward, I., and R. Jackson, *ibid.*, **20**, 911 (1965).
5. Fan, L. T., "The Continuous Maximum Principle," John Wiley, New York (1966).
6. Fine, F. A., and S. G. Bankoff, *Ind. Eng. Chem. Fundamentals*, **6**, 288 (1967).
7. Lasdon, L. S., et. al., *Trans. Auto. Control*, **AC-12**, 132 (1967).
8. Mangasarian, O. L., *J. SIAM. Control*, **4**, 139 (1966).
9. McSwain, C. V., and L. D. Durbin, *Separation Sci.*, **1**, 677 (1966).
10. Pontryagin, et. al., "The Mathematical Theory of Optimal Processes," MacMillan, New York (1964).
11. Rosenbrock, H. H., and C. Storey, "Computational Techniques for Chemical Engineers," Pergamon Press, Oxford (1966).
12. Wilde, D. J., and C. S. Beightler, "Foundations of Optimization," Prentice-Hall, Englewood Cliffs, N. J. (1967).